2022 US-Japan Seminar on Dielectric and Piezoelectric Ceramics
Charleston, South Carolina
November 13 - 16, 2022

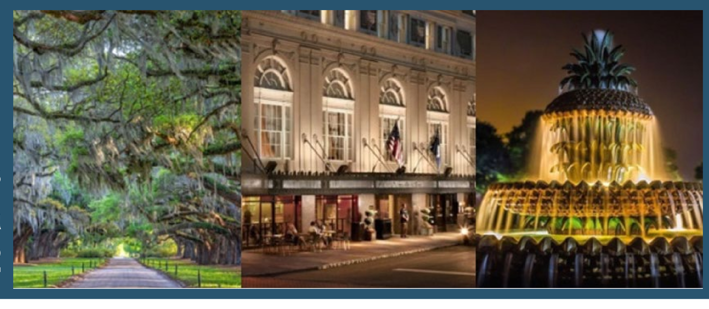

Dielectric Stimulated Arc Breakdown Across a Spark Gap for Surge Protection

Pin Yang*[1], John K. Grey[2], David E. Vreeland[3], and Josef D. Sorenson[1]
*[1]Electronic, Optical, and Nano Materials, [2]Organic Materials Science, [3]Connectors and LACs
Sandia National Laboratories, Albuquerque, New Mexico 87155, USA

The introduction of high dielectric permittivity ceramic granules in a spark gap geometry can divert surge currents by significantly reducing the breakdown voltage and narrowing its distribution. This work demonstrates a practical application for surge protection and reviews basic concepts of dielectric stimulated arc breakdown at lower voltages. Key factors such as dielectric constant and gas pressure on the fast-rise breakdown in a dielectric filled spark gap will be reported and discussed.

1. INTRODUCTION

High power surges can pose a serious threat to electrical systems. Effective diversion of power surges is vital to prevent unwanted damage to sensitive electronics. Dielectric stimulated arc breakdown is a fast, effective, and self-healing mechanism that can quickly divert unexpected surges to ground and mitigate damage. The mechanism lowers the breakdown threshold voltage and current density since the resistance of the arc plasma increases with decreasing electric potential.

This paper reviews the basic concepts of dielectric stimulated arc breakdown across a spark gap and demonstrates the importance of dielectric permittivity of ceramic granules in lowering the breakdown voltage for surge protection. Effects of gas pressure on the arc breakdown will be also reported.

1.1 Paschen Breakdown

Arc breakdown due to discharge across an air gap is governed by the ability to ionize gas molecules under the influence of an electric field according to the Paschen's law. The breakdown voltage with respect to the product of gap width (d) and pressure (p) is generally referred as the Paschen curve.. Scenarios and relative electron mean free paths (l_e) are illustrated in these insert drawings in Fig. 1.

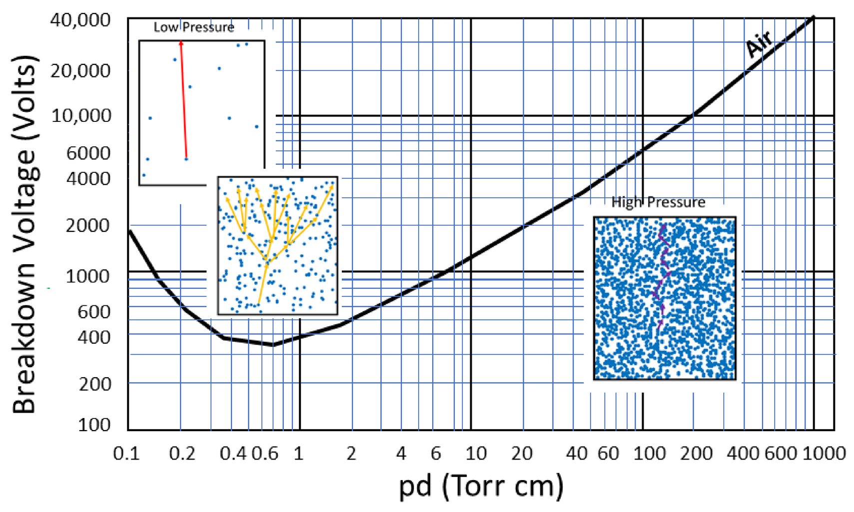

Fig. 1. Paschen curve of air under ambient temperature. The blue dots and arrows are representing the gas molecules and l_e, respectively.

1.2 Field Splitting due to Dielectric Insertion

The insertion of a higher permittivity dielectric to the air gap concentrates the electric field across the air gap. Since. the total charge (Q) at the air and dielectric interface under applied voltage (V_{total}) remains the same, so

$$Q = C_{Air}V_{Air} = C_{Dielectric}V_{Dielectric},$$

Since E = V/d; therefore, most field or voltage will be concentrated in the air ($\varepsilon'_{Air} = 1$)

$$E_{Air}\,\varepsilon'_{Air} = E_{Dielectric}\,\varepsilon'_{Dielectric}$$

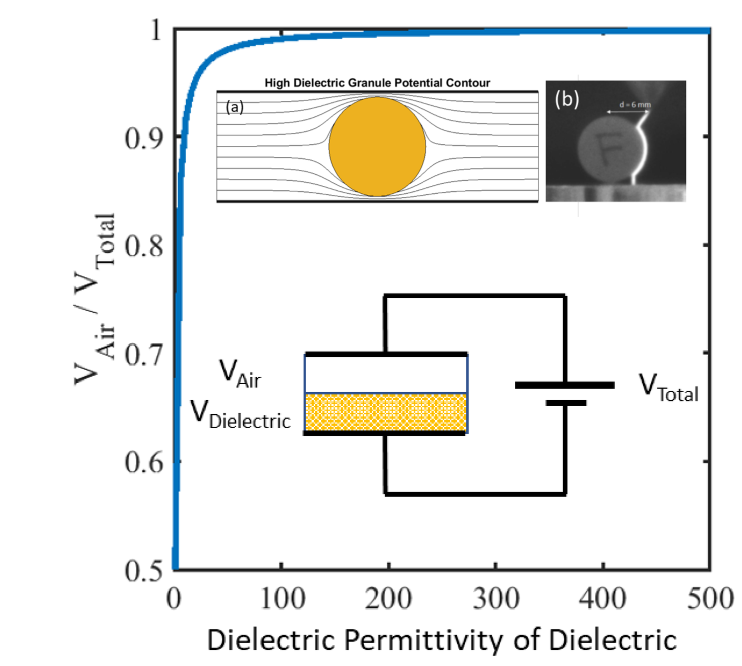

Fig. 2. Change of voltage (or electric field) distribution as a function of dielectric permittivity of the inserted dielectric based on a simple parallel plate capacitor. Top inserts show (a) distortion of isopotential lines, (b) field distortion on arc breakdown path due to the introduction of high permittivity of dielectric granules.

2.EXPERIMENTAL PROCEDURE

Fast-rise breakdown (FRB) was measured by an amplified square pulse > 1200V with 300 ns to 1 μs pulse width. The voltage ramp rate was adjusted by a pulse shaping network to be as close as possible to 10 kV/μs to simulate a fast rising surge condition. Traces of the trigger pulse and voltage waveform across the PMN-PT granule filled spark gap were digitally recorded by an oscilloscope (Agilent, Infini Vision DSO6054A) and analyzed by a MATLAB program. The maximum surge voltage and voltage ramp rate were determined from voltage/current waveforms of 21 consecutive shots to ensure statistical reliability and average values and standard deviation were compared and analyzed. For temperature dependent measurements, breakdown data were collected continuously with a five-second interval between each shot to de-energize and relax residual ionized species between the spark gap.

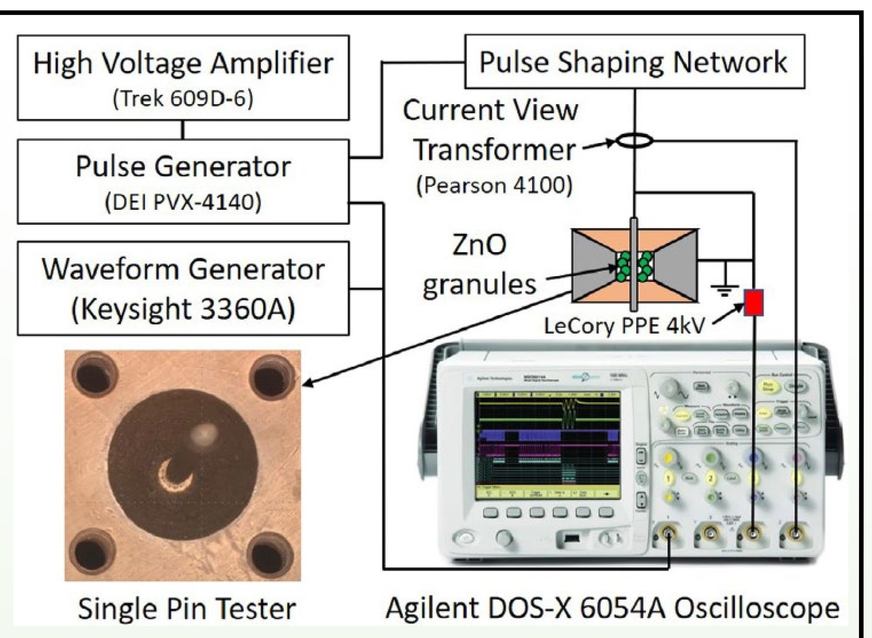

Fig. 3. Schematic diagram of he fast-rise breakdown measurement system.†

† P. Yang et al., J. Am. Ceram. Soc., 2020.

FAST RISE BREAKDOWN AND WAVEFORM

Typical FRB waveforms including the voltage and the current traces for a PMN-PT filled spark gap are illustrated in Fig. 4. The FRB is distinguished by a quick linear rising potential to the peak voltage (V_B) followed by sharp decrease and change of sign as shown in Fig. 4(a). The hallmark of a dielectric induced arc breakdown is further confirmed by comparing the current response (Fig. 4 (b)) where a large current spike at breakdown initiation (voltage drop) consistent with complete gas discharge.

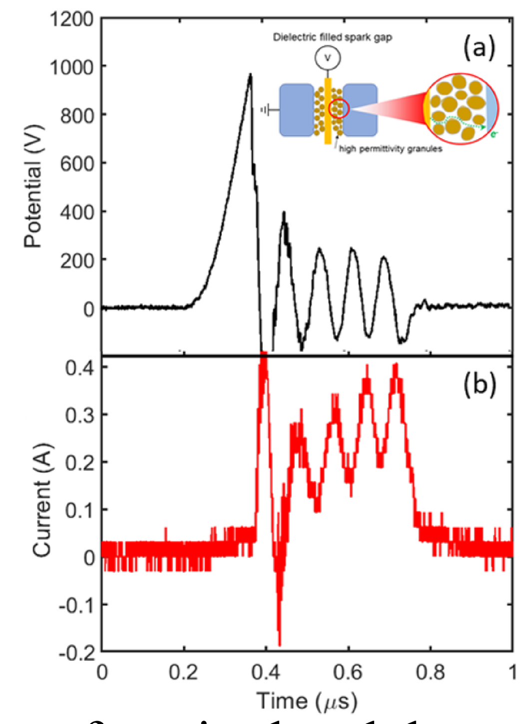

Fig. 4. (a) Voltage and (b) current waveforms obtained from a fast-rise breakdown,

PASCHEN CURVE OF DIELECTRIC FILLED SPARK GAP

The shape of the Paschen curve is similar to Fig. 1, except the V_B is lower so the change in V_B with respect to pressure in the mechanistically limited region is much steeper. Due to the limitation imposed by l_e in the mechanistically limited region, the standard deviation of the breakdown voltage is smaller than data collected in the stochastic range on the right. Data indicate that near ambient condition V_B for the annulus spark gap is about 1150±45 V, and the Paschen minimum is around 25 Torr.

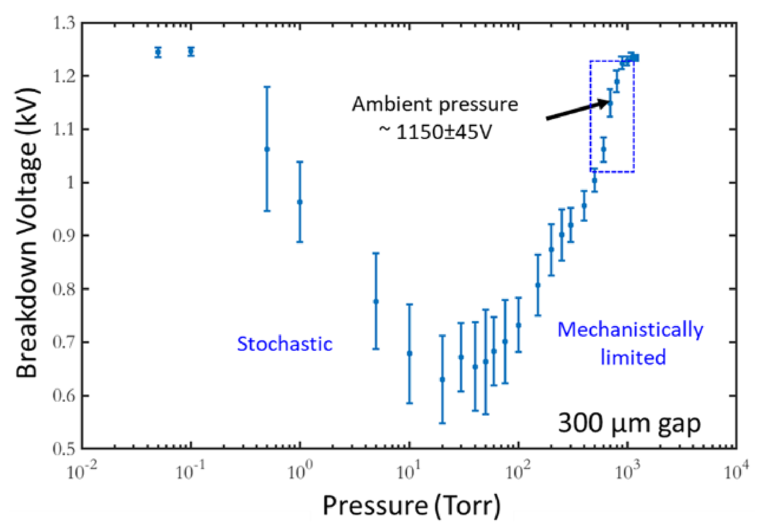

Fig.5 Paschen behavior of PMN-PT granules filled spark gap.

The results indicate that the breakdown response of a dielectric filled spark gap is still governed by the same mechanisms described by Paschen's law.

DIELECTRIC CONSTANT AND BREAKDOWN VOLTAGE

The change of V_B and ε' (10 kHz) versus temperature for the PMN-PT were plotted on the left and right Y axis in Fig. 6, respectively. The result shows the Curie temperature (T_c) is at 252° C. Two sets of V_B data show a similar trend which decreases monotonically to the minimum point at the T_c, then increases as temperature increases. The general up shift in the breakdown voltage is consistent with Paschen's law in the mechanistically limited region (Fig. 5).

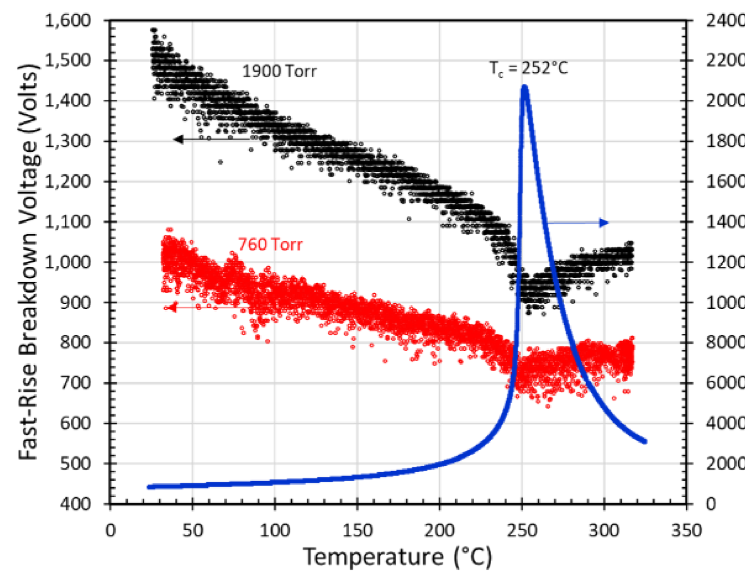

Fig. 6. Temperature dependence of V_B and e for PMN-PT granule filled spark gap and pellet.

DIELECTRIC ENHANCED BREAKDOWN

The change of V_B with respect to the ε' of PMN-PT under three different pressure conditions is given in Fig. 7. The dielectric data are compiled from the temperature dependent measurements on both sides of the Curie point on Fig. 6. These curves illustrate the effect of field concentration due to dielectric constant change to the V_B. The shape of these curves is unique to the annulus shape test fixture, and may vary with the shape, size and distribution of dielectric granules.

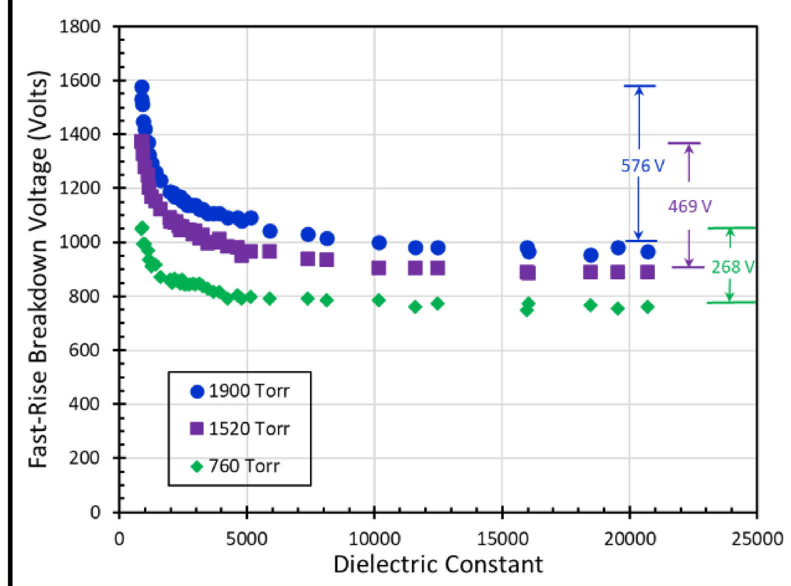

Fig. 7. Change in V_B versus ε' of PMN-PT under different pressures.

CONCLUDING REMARKS:

From the change of dielectric constant of PMN-PT as a function of temperature and the change of V_B with respect to pressure, an important correlation of high permittivity granules on arc breakdown in a spark gap is demonstrated, which serves as the technical basis for surge protection design. The arc breakdown of a dielectric filled spark gap still follows the Paschen's law with a breakdown minimum below the ambient pressure. Results indicate that the extent of field concentration due to the introduction of the high permittivity granules dictates the minimum breakdown voltage.

Sandia National Laboratories is a multimission laboratory managed and operated by National Technology & Engineering Solutions of Sandia, LLC, a wholly owned subsidiary of Honeywell International Inc., for the U.S. Department of Energy's National Nuclear Security Administration under contract DE-NA0003525.
SAND No. ___________